Journal of Harbin Engineering University
ISSN: 1006-7043

Vol 45 No. 3
March 2024

Optimizing Downforce: The Role of Diffuser Angle in Open-Wheeled Race Car Aerodynamics

[1]Sadan Kanchanapalli, [1]Akhil Jalagam, [1]Ashvin Dandothkar, [1]Dr. B. Ravi Kumar

[1]Maturi Venkata Subba Rao (MVSR) Engineering College, Hyderabad, India

All Authors Have Contributed Equally

***Corresponding Author:** Sadan Kanchanapalli

*Maturi Venkata Subba Rao (MVSR) Engineering College, Hyderabad, India

Abstract

This study investigates the aerodynamic performance of an open-wheeled race car through Computational Fluid Dynamics (CFD) simulations, with a specific focus on the diffuser angle. The decision to adopt a 10° diffuser angle is justified by its potential to maximize downforce generation while considering trade-offs with other performance parameters. Through meticulous evaluation of various diffuser angles, the selected angle demonstrates an optimal balance between downforce gains and potential drawbacks, highlighting the importance of meticulous aerodynamic configuration for enhancing race car performance.

Keywords: Aerodynamics, Computational Fluid Dynamics (CFD), Open-wheeled race car, Diffuser angle, Downforce, Performance evaluation, Optimization, Trade-offs, Aerodynamic configuration, Race car performance, Fédération Internationale de l'Automobile (FIA).

1. Introduction

Open-wheeled race cars are high-performance vehicles designed for competitive racing events, where precision, speed, and aerodynamics play pivotal roles. These specialized machines are characterized by their exposed wheels, which are not covered by fenders or bodywork, contributing to their distinctive and aerodynamically efficient design. Open-wheel racing is a popular and prestigious form of motorsport, attracting skilled drivers and passionate fans worldwide.

1.1 Components of Open-Wheeled Race Cars:

An exploded view of an F1 race car offers a detailed breakdown of its components, providing insight into its intricate design. The chassis forms the structural foundation, while the power unit drives propulsion. Suspension systems ensure stability, aerodynamics optimize performance, and bodywork provides both protection and aerodynamic efficiency. Cooling systems manage engine temperatures, transmissions transfer power, electronics control various functions, braking systems ensure safe deceleration, and fuel systems deliver fuel efficiently. This visualization reveals the complexity behind the high-performance dynamics of an F1 car.

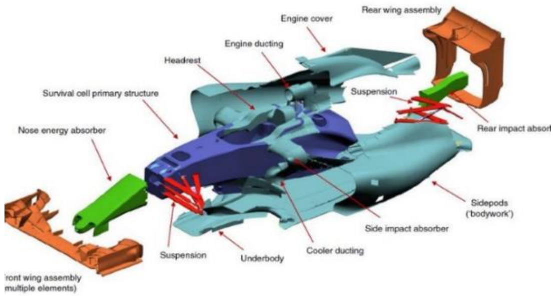

Fig 1: Exploded View of an F1 Car

1.2 Types of Rear Diffusers:

Rear diffusers in open-wheel race cars come in various types. The single-element diffuser is a basic design featuring a single curved element, providing moderate downforce. It is commonly seen in entry-level racing categories.

Multi-element diffuser incorporates multiple channels or fins, increasing downforce levels compared to the single-element design. It is typically used in mid-tier racing series.

Double deck diffuser boasts two levels of elements, delivering significant downforce. This advanced design is often employed in top-tier racing competitions.

Gurney flap, a small vertical element added to the rear wing, offers adjustability to enhance downforce and reduce drag. It is adaptable for various track conditions.

Swan neck diffuser stands out with its unique design, where the rear wing supports connect to the top surface. This optimizes airflow for improved overall performance.

2. Objective

This Paper aims to develop and implement an innovative multi-element diffuser tailored for open-wheel race cars, with a focus on enhancing both downforce generation and overall aerodynamic efficiency. By employing advanced aerodynamic design principles, the objective is to significantly improve traction, stability, and cornering capabilities of the race car, through the manipulation of airflow and pressure differentials, the aim is to maximize the diffuser's effectiveness in generating downforce for formula 3 race car as per FIA Guidelines. To achieve this goal, cutting-edge engineering principles and state-of-the-art technologies are integrated into the design and implementation process. Ultimately, the project endeavours to elevate the competitive edge and performance potential of open-wheel race cars in motorsport competitions, pushing the boundaries of innovation in aerodynamic design.

3. Modelling and Analysis

3.1 Dimensions of Bluff Body and Diffuser:

According to the technical regulations outlined by the FIA for Formula 3 cars, specific rules govern the design of the Formula 3 Vehicle. According to the regulations set by the FIA, the bluff body employed is with a total length of 3350mm, a total height of 960mm, and a width of 1000mm. The diffuser length is 500mm, and its angle is varied between 8° and 30°. The wheelbase of the bluff body is taken as 3000mm, and the diffuser starts 150mm behind the rear wheel centre line.

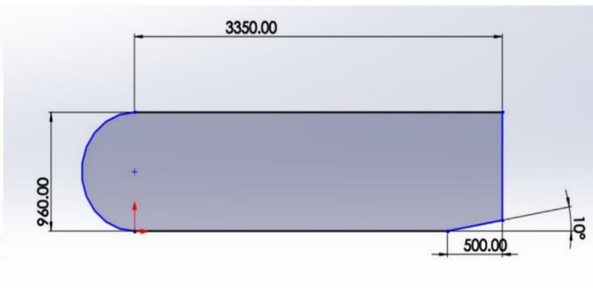

Fig 2: Dimensions of Diffuser Geometry

3.2 Diffuser CFD Analysis:

To determine the critical conditions for designing a diffuser, computational fluid dynamics (CFD) analysis is conducted on various test cases. These test cases involve different combinations of ride heights, diffuser angles, and speeds. Specifically, ride heights of 20, 30, 50, 70, and 90mm are selected, along with diffuser angles ranging from 8° to 30°. Speeds considered for analysis are 20, 30, 40, and 50 m/s. Boundary conditions are established within the computational domain to simulate realistic scenarios. The velocity inlet is positioned 2500mm from the front wheel centre line, with a length of 4000mm. A pressure outlet is employed with the same length as the velocity inlet at a position of 6000mm behind the front wheel centre line. The upper boundary of the bluff body is treated as a free slip wall with a length of 8500mm, while the lower boundary is defined as a no slip wall imitating the conditions of the road, also extending 8500mm. These boundary conditions ensure that the CFD analysis captures relevant flow phenomena and informs the design of an effective diffuser for the Formula 3 car.

3.3 CFD Analysis:

The fluid domain for the computational analysis was meshed using the Ansys Fluent Meshing tool. For inflation, which aids in capturing boundary layer effects, a smooth transition ratio of 0.2 was utilized. Eight layers were generated to ensure adequate resolution near the surfaces, with a growth rate of 1.1 to maintain layer thickness consistency. Sizing parameters were set to achieve the desired mesh density, with a size of 5e-4 meters for the elements. A "harder" behaviour was implemented to prioritize mesh quality, ensuring accurate representation of flow features. Additionally, the overall mesh size was defined as 5e-2 meters to balance computational efficiency with solution accuracy. The total nodes obtained after the meshing are 281314 and the total elements obtained are 272336.

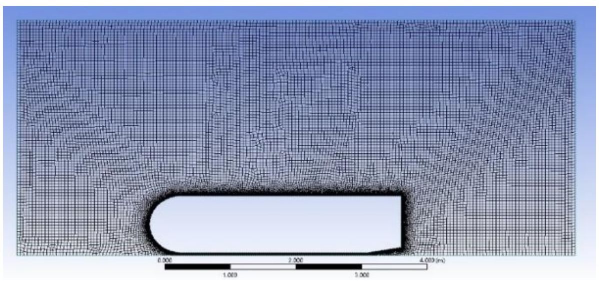

Fig 3: Domain Mesh

3.3 CFD Solver:

The selection of the SST k-omega turbulence model for solving the chosen test cases was driven by its notable advantages in accuracy, especially when dealing with boundary layers and modelling near surfaces. The SST (Shear-Stress Transport) model combines elements of both k-epsilon and k-omega models, making it well-suited for capturing the intricacies of turbulence in complex flow situations. In scenarios with boundary layers, where the flow near surfaces is critical, the SST k-omega model has demonstrated superior performance compared to other turbulence models. Its ability to provide more accurate solutions in such conditions makes it a preferred choice for researchers and engineers seeking reliable and precise results in computational fluid dynamics.

4. Results

The Result is obtained by solving the solution with 1000 iterations for obtaining a converging solution and the time taken for computation in the system having specifications of a CPU Clock speed of 2.3 GHz and a RAM of 32GB is around 1 hour without considering the time for meshing. The Results are as follows.

4.1 Simulation Results:

The Results obtained are shown graphically in the figures given below.

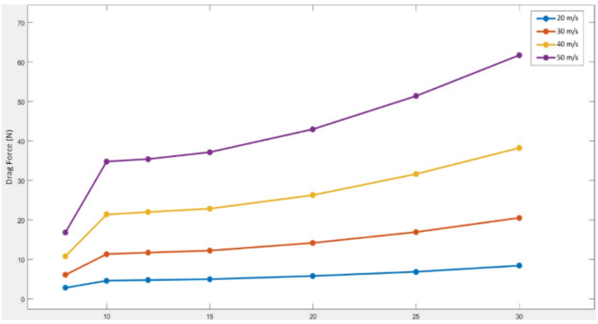

Fig 4: Drag [N] v/s Diffuser Angle

Fig 4 analysis reveals a clear pattern that drag force increases with higher speeds and diffuser angles. This suggests a correlation between diffuser angle and drag force, with higher speeds exacerbating drag due to increased air resistance. The graph underscores the sensitivity of the system to these variables, offering insights into aerodynamic behaviour.

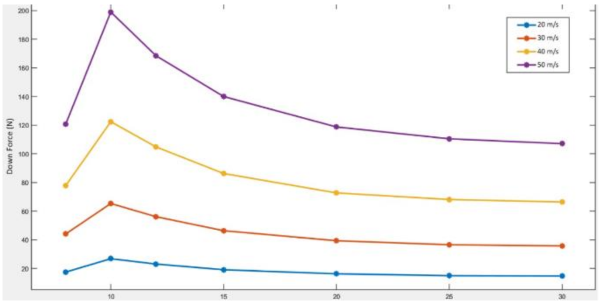

Fig 5: Downforce [N] v/s Diffuser Angle

Fig 5 analysis shows a distinct trend, as diffuser angle increases, downforce rapidly rises but eventually diminishes beyond a critical point. This suggests an optimal angle exists for maximizing downforce. The phenomenon is consistent across speeds, indicating a general system behaviour. Optimizing diffuser angle is crucial for achieving maximum downforce.

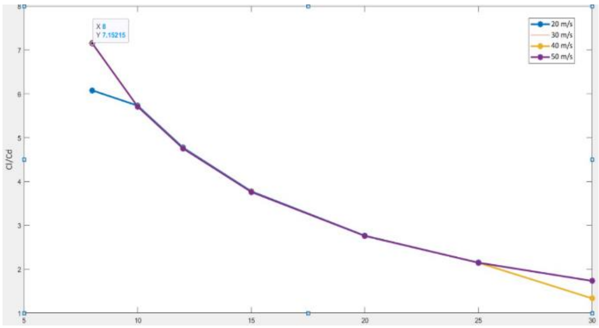

Fig 6: Cl/Cd v/s Diffuser Angle

Fig 6 indicates a consistent trend, as diffuser angle increases, the ratio of lift coefficient to drag coefficient (cl/cd) decreases. This suggests improved aerodynamic efficiency with higher diffuser angles, as seen in reduced Cl and Cd values. Despite speed variations, the changes in Cl/Cd values are not significant, implying the optimized diffuser angle is effective across speeds. Overall, increasing diffuser angle decreases Cl/Cd, highlighting enhanced aerodynamic performance.

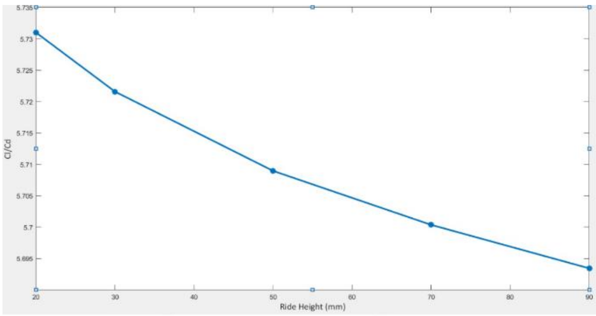

Fig 7: Cl/Cd v/s Ride Heights

Fig 7 indicates a consistent trend. From the graph it is observed that, as ride height increases the ratio of lift coefficient to drag coefficient (cl/cd) has a negligible decrease across different speeds. This suggests that the higher ride heights lead to less efficient aerodynamics as seen through the declining of cl/cd ratio even though it is negligible. The trend in this Fig 8 holds regardless of speed.

4.2 Pressure Contours:

The Pressure contours obtained have a low pressure in the underbody where the diffuser starts the velocity of the air increases decreasing the pressure in the underside of the body. The Pressure contours show the same trend across all the test cases and the pressure contours for the critical diffuser setup has been shown below at different speeds.

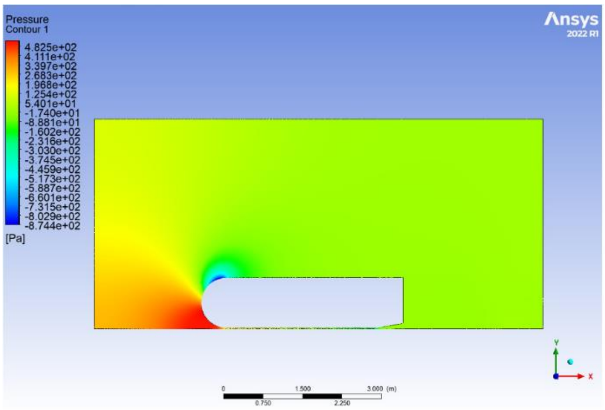

Fig 8: Pressure contour at 10° diffuser angle, 20m/s speed, and 20mm ride height

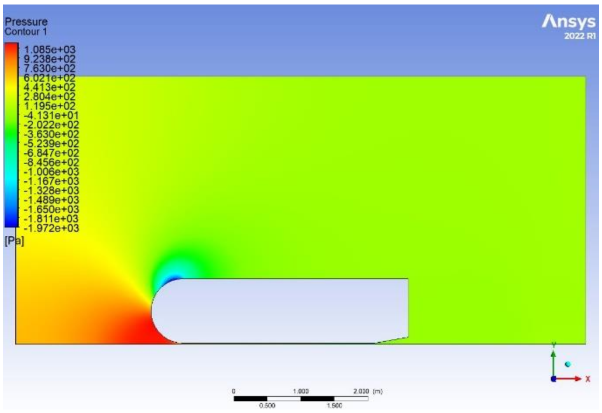

Fig 9: Pressure contour at 10° diffuser angle, 30m/s speed, and 20 mm height

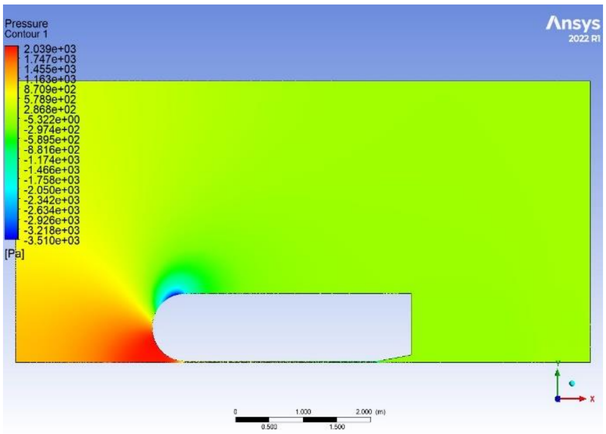

Fig 10: Pressure contour at 10° diffuser angle, 40m/s speed, and 20 mm height

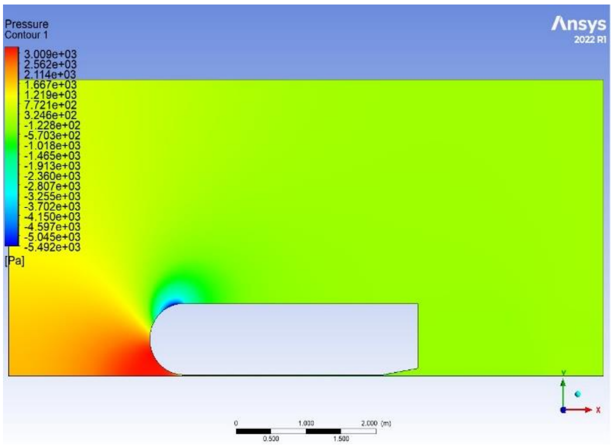

Fig 11: Pressure contour at 10° diffuser angle, 50m/s speed, and 20 mm height

4.2 Velocity Contours:

The velocity contours obtained show an increase of velocity at the diffuser location and a boundary layer is formed on the diffuser. The velocity in the underbody increases as the pressure in the underside of the body is decreasing consistently. The Velocity contours show the same trend across all the test cases and the velocity contours for the critical diffuser setup has been shown below at different speeds.

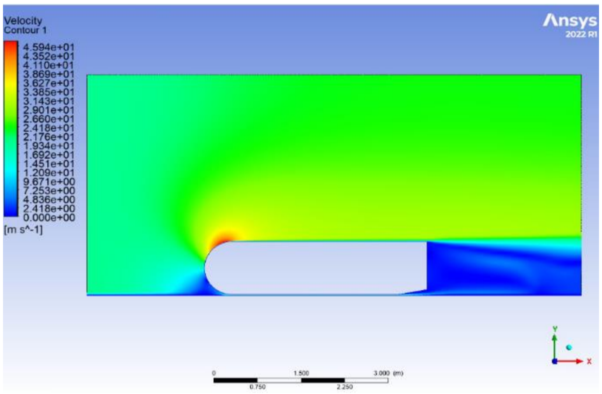

Fig 12: Velocity contour at 10° diffuser angle, 20m/s speed, and 20 mm height

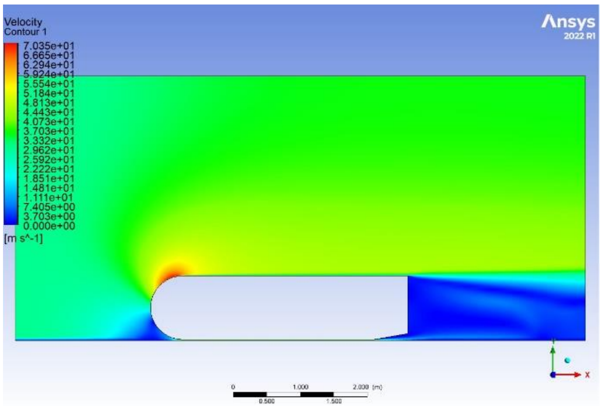

Fig 13: Velocity contour at 10° diffuser angle, 30m/s speed, and 20 mm height

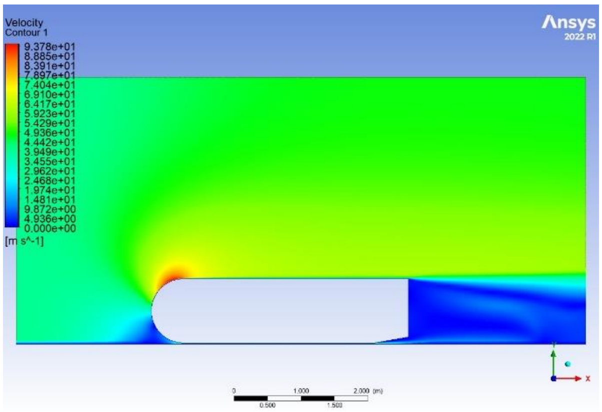

Fig 14: Velocity contour at 10° diffuser angle, 40m/s speed, and 20 mm height

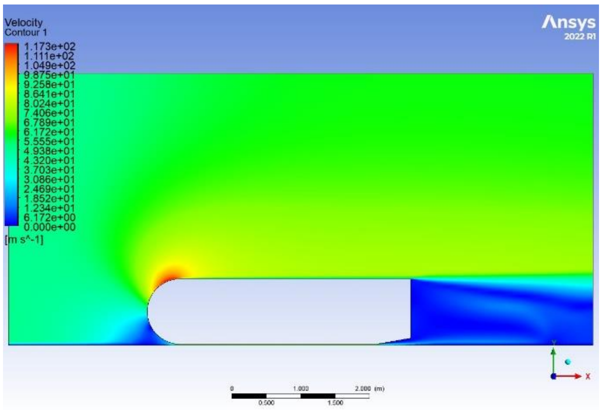

Fig 15: Velocity contour at 10° diffuser angle, 50m/s speed, and 20 mm height

Table 1 Simulation Results for varying diffuser angles

S.No.	Ride Height (mm)	Diffuser Angle (deg)	Speed (m/s)	Down Force (N)	Drag Force (N)	Cl	Cd	Cl/Cd
1	20	8	50	120.60061	16.862143	0.157519164	0.022024024	7.152152013
2	**20**	**10**	**50**	**198.90601**	**34.843296**	**0.259795605**	**0.045509611**	**5.708587672**
3	20	12	50	168.44905	35.445334	0.220015086	0.046295946	4.752361764
4	20	15	50	139.95406	37.196349	0.18279714	0.048582986	3.762575193
5	20	20	50	118.70687	43.014945	0.155045708	0.056182785	2.759665739
6	20	25	50	110.42939	51.413012	0.144234305	0.067151689	2.14788797
7	20	30	50	107.0379	61.748344	0.139804604	0.080650898	1.733453775

Table 2 Simulation Results for Varying Ride Height

S.No.	Ride Height (mm)	Diffuser Angle (deg)	Speed (m/s)	Down Force (N)	Drag Force (N)	Cl	Cd	Cl/Cd
1	20	10	20	26.760414	4.6694071	0.218452359	0.038117609	5.731008975
2	30	10	20	48.62476	8.4984661	0.396936816	0.069375233	5.721592512
3	50	10	20	74.416652	13.03504	0.607482873	0.10640849	5.708969976
4	70	10	20	85.309099	14.965527	0.696400808	0.122167567	5.700373866

5	90	10	20	101.11924	17.760638	0.825463184	0.1449848	5.693446373

Table 3 Experimental Results for Varying Velocities

S.No.	Ride Height (mm)	Diffuser Angle (deg)	Speed (m/s)	Down Force (N)	Drag Force (N)	Cl	Cd	Cl/Cd
1	20	10	20	26.760414	4.6694071	0.218452359	0.038117609	5.731008975
2	20	10	30	65.256204	11.407463	0.236757203	0.041387621	5.720483512
3	20	10	40	122.36818	21.420574	0.24973098	0.043715457	5.712647103
4	20	10	50	198.90601	34.843296	0.259795605	0.045509611	5.708587672

4.3 Selection of 10° Diffuser Angle:

The primary goal of enhancing the downforce on an open-wheeled race car has been a crucial consideration, and the analysis has revealed that among various diffuser angles, the maximum downforce is achieved at a 10° diffuser angle. This observation leads to the decision to select a 10° diffuser angle as it yields the highest downforce performance.

The choice of a 10° diffuser angle is based on careful examination of the relationship between diffuser angle and downforce generation. The analysis conducted indicates that as the diffuser angle increases, the downforce progressively rises until it reaches a peak at 10° as shown in table 1. Beyond this angle, further increases may not result in a proportional gain in downforce and could potentially lead to diminishing returns.

Selecting and identifying the 10° diffuser angle as the critical angle aligns with the objective of maximizing downforce while maintaining an optimal balance with other aerodynamic considerations. This decision is the result of a trade-off between achieving higher downforce levels and avoiding excessive drag and other aerodynamic penalties associated with extreme diffuser angles.

In summary, the decision to choose a 10° diffuser angle is grounded in the pursuit of maximizing downforce for the open-wheeled race car for selected geometry. This choice reflects a careful evaluation of the performance characteristics at different angles and emphasizes the importance of balancing downforce gains with potential drawbacks to achieve an optimal overall aerodynamic configuration.

5. Conclusion

In conclusion, the meticulous analysis and design process outlined in this study have culminated in the development of an innovative multi-element diffuser for open-wheel race cars, aimed at enhancing downforce generation and overall aerodynamic efficiency. Through comprehensive CFD analysis, experimentation with diffuser angles, and adherence to FIA regulations, a 10° diffuser angle has been identified as optimal for maximizing downforce while minimizing drag. The maximum value obtained for downforce at 10° diffuser angle, 20mm ride height and at a velocity of 50m/s is 198.90601N. Future experimental validation and iterative optimization efforts are poised to further refine the diffuser design, ultimately elevating the competitive edge and performance potential of open-wheel race cars in motorsport competitions.

References

[1] Kishore, R., Nivethan, M. H., Khumar, S. P., & Bharathi, A. A. (2022, November). 'Design and CFD analysis of undertray diffuser for formula student cars': In AIP Conference Proceedings (Vol. 2446, No. 1). AIP Publishing.

[2] Yew, L. W., Al-Obaidi, A. S. M., & Namasivayam, S. (2017). 'Design and Development of a Multi-Element Active Aerodynamic Package to Enhance the Performance of Taylor's Formula SAE Car': In International Engineering Research Conference (8th Eureca).

[3] Calişkan, m., & bakirci, a. (2022). An investigation of the different diffuser positions effect on vehicle aerodynamic performance. International journal of automotive science and technology, 6(1), 75-82.

[4] Augue Peddie, K. M., & Gonzalez, L. F. (2009). CFD Analysis of the Diffuser of a Formula 3 Race car. Orbit: University of Sydney Undergraduate Research Journal, 1(1).

[5] Mahon, S. A. (2005). The aerodynamics of multi-element wings in ground effect

(Doctoral dissertation, University of Southampton).

[6] Willemsen, D. H. J. (2012). CFD-based aerodynamic optimisation of a 2D race car diffuser. Eindhoven University of Technology, pág, 8-19.

[7] Tuttle, J. L., & Blount, D. H. (1983). Perfect bell nozzle parametric and optimization curves (No. NASA-RP-1104).

[8] Alkan, B. (2013). Aerodynamic Analysis of Rear Diffusers for a Passenger Car Using CFD.

[9] Guerrero, A., Castilla, R., & Eid, G. (2022). A numerical aerodynamic analysis on the effect of rear underbody diffusers on road cars. Applied Sciences, 12(8), 3763.

[10] Abid, M., Wajid, H. A., Iqbal, M. Z., Najam, S., Arshad, A., & Ahmad, A. (2017). Design and analysis of an aerodynamic downforce package for a Formula Student Race Car. IIUM Engineering Journal, 18(2), 212-224.

[11] Poutiainen, A. (2021). Undertray Design and Development Procedure with CFD: An Optimization Study of Different Undertray Designs with CFD Computations.

[12] Ehirim, O. H., Knowles, K., & Saddington, A. J. (2019). A review of ground-effect diffuser aerodynamics. Journal of Fluids Engineering, 141(2), 020801.

[13] Das, S. K., Kumar, P., & Rawat, S. (2013). Alterations of formula 3 race car diffuser geometry for optimized downforce. Int. J. Eng. Res. Tech., 6(3), 351-358.

[14] BHARDWAJ, A. Analysis of Ground Effect Diffuser on a Race Car to Optimize Aerodynamic Performance.

[15] Khokhar, A. A. S., & Shirolkar, S. S. (2015). Design and analysis of undertray diffuser for a formula style race car. International Journal of Research in Engineering and Technology, 4(11), 202-210.

[16] Ekman, P. (2020). Important Factors for Accurate Scale-Resolving Simulations of Automotive Aerodynamics (Vol. 2068). Linköping University Electronic Press.

[17] Knight, J., Spicak, M., Kuzenko, A., Haritos, G., & Ren, G. (2019). 'Investigation of vehicle ride height and diffuser diffuser angle on downforce and efficiency': In Proceedings of the Institution of Mechanical Engineers, Part D: Journal of Automobile Engineering, 233(8), 2139-2145.

[18] de Wilde, W., Gunnarsson, J., Ivarsson, L., Karlsson, L., Kolte, O., & Olander, D. (2021). Development and performance evaluation of undertray diffusers during racing manoeuvres.

[19] Jørgensen, S. M. Numerical Investigation of a diffuser equipped bluff body using student-level resources.

[20] Katz, J., & Garcia, D. (2002). Aerodynamic effects of Indy car components. SAE Transactions, 2322-2330.

[21] Biswal, S., Prasanth, A., & Naranje, V. G. (2016). 'Design and Optimization of the Diffuser for the Formula SAE Car for Improved Performance': In Proceedings of the World Congress on Engineering (Vol. 2).